

Mutation of Nicotinamide Pocket Residues in Rat Liver 3 α -Hydroxysteroid Dehydrogenase Reveals Different Modes of Cofactor Binding[†]

Haiching Ma,[§] Kapila Ratnam,^{||} and Trevor M. Penning*

Department of Pharmacology, University of Pennsylvania, School of Medicine, 3620 Hamilton Walk, Philadelphia, Pennsylvania 19104-6084

Received July 19, 1999; Revised Manuscript Received October 18, 1999

ABSTRACT: Rat liver 3 α -hydroxysteroid dehydrogenase (3 α -HSD), an aldo–keto reductase, binds NADP⁺ in an extended *anti*-conformation across an (α/β)₈-barrel. The orientation of the nicotinamide ring, which permits stereospecific transfer of the 4-*pro-R* hydride from NAD(P)H to substrate, is achieved by hydrogen bonds formed between the C3-carboxamide of the nicotinamide ring and Ser 166, Asn 167, and Gln 190 and by π -stacking between this ring and Tyr 216. These residues were mutated to yield S166A, N167A, Q190A, and Y216S. In these mutants, $K_d^{\text{NADP(H)}}$ increased by 2–11-fold but without a significant change in $K_d^{\text{NAD(H)}}$. Steady-state kinetic parameters showed that $K_m^{\text{NADP}^+}$ increased 13–151-fold, and this was accompanied by comparable decreases in $k_{\text{cat}}/K_m^{\text{NADP}^+}$. By contrast, $K_m^{\text{NAD}^+}$ increased 4–8-fold, but changes in $k_{\text{cat}}/K_m^{\text{NAD}^+}$ were more dramatic and ranged from 23- to 930-fold. Corresponding changes in binding energies indicated that each residue contributed equally to the binding of NADP(H) in the ground and transition states. However, the same residues stabilized the binding of NAD(H) only in the transition state. These observations suggest that different modes of binding exist for NADP(H) and NAD(H). Importantly, these modes were revealed by mutating residues in the nicotinamide pocket indicating that direct interactions with the 2'-phosphate in the adenine mononucleotide is not the sole determinant of cofactor preference. The single mutations were unable to invert or racemize the stereochemistry of hydride transfer even though the nicotinamide pocket can accommodate both *anti*- and *syn*-conformers once the necessary hydrogen bonds are eliminated. When 4-*pro-R*-[³H]NADH was used to monitor incorporation into [¹⁴C]-5 α -dihydrotestosterone, a decrease in the ³H:¹⁴C ratio was observed in the mutants relative to wild-type enzyme reflecting a pronounced primary kinetic isotope effect. This observation coupled with the change in the binding energy for NAD(P)(H) in the transition state suggests that these mutants have altered the reaction trajectory for hydride transfer.

Hydroxysteroid dehydrogenases (HSDs) play pivotal roles in the biosynthesis and inactivation of all steroid hormones. They belong to two protein families: the short-chain dehydrogenases/reductases (SDRs) and the aldo–keto reductases (AKRs). Members of both families use nicotinamide cofactors for the stereospecific oxidoreduction of steroid hormones but possess structurally different binding domains for the cofactor. SDRs are multimeric and contain a Rossmann fold for binding the nucleotide cofactor (1). In

this family, the nicotinamide ring lies in an extended *syn*-conformation with respect to the ribose ring and the 4-*pro-S* hydrogen is transferred to the substrate. Crystallographic studies of SDRs bound with NAD⁺ indicate that the enzyme forms one or two hydrogen bonds with the C3-carboxamide group to lock the orientation of the nicotinamide ring in position (2, 3). By contrast, AKRs are monomeric and have an (α/β)₈-barrel motif (4, 5). The nicotinamide ring adopts an *anti*-conformation, and the enzyme catalyzes the transfer of the 4-*pro-R* hydrogen to the substrate (6–9).

Rat liver 3 α -HSD (EC 1.1.1.213) is the most extensively characterized HSD in the AKR superfamily with an ordered kinetic mechanism in which pyridine nucleotide binds first and leaves last (9). Its principal physiological role is to inactivate circulating androgens, progestins, and glucocorticoids. In the human prostate, 3 α -HSD isoforms catalyze the conversion of the potent androgen 5 α -dihydrotestosterone (5 α -DHT) to the weaker androgen 3 α -androstenediol and regulate occupancy of the androgen receptor (10). It has been recently shown that type 2 3 α (17 β)-HSD in human prostate eliminates 5 α -DHT from this tissue (11). Virtually all mammalian 3 α -HSDs are AKRs, and structure–function studies on the rat liver enzyme are pertinent to the biologically important human isoforms.

[†] This work was supported by NIH Grant DK47015 to T.M.P., and H.M. was partially supported by NIH Predoctoral Training Grant in Pharmacology.

* To whom correspondence should be addressed. Tel: (215) 898-9445. Fax: (215) 573-2236. E-mail: penning@pharm.med.upenn.edu.

[§] Current address: Institute for Medicine & Engineering, 1150 Vagelos Bldg, University of Pennsylvania, Philadelphia, PA 19104-6383.

^{||} Current address: SmithKline Beecham Pharmaceuticals, UP1345, Collegeville, PA 19426.

¹ Abbreviations: HSD, hydroxysteroid dehydrogenase; 3 α -HSD, 3 α -hydroxysteroid dehydrogenase or 3 α -hydroxysteroid-NAD(P)⁺-oxidoreductase (formerly EC 1.1.1.50 and now EC 1.1.1.213 because of its A-face specificity in hydride transfer, now also designated AKR1C9); AKR, aldo–keto reductase; 5 α -DHT or 5 α -dihydrotestosterone, 17 β -hydroxy-5 α -androstane-3-one; androsterone, 3 α -hydroxy-5 α -androstane-17-one; androstenedione, 5 α -androstane-3,17-dione.

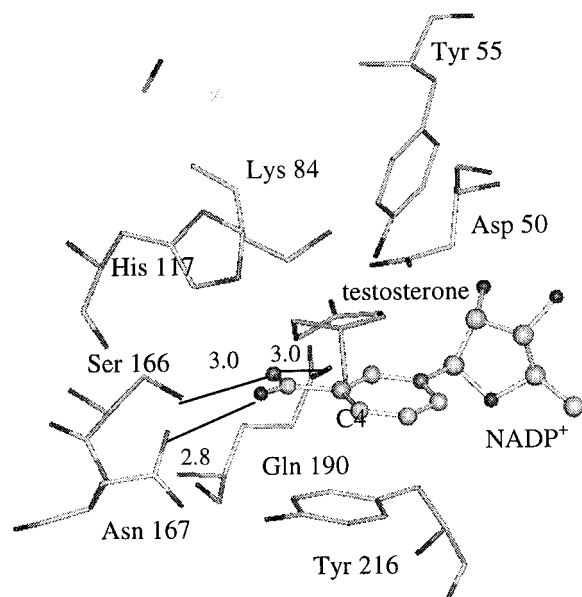


FIGURE 1: Atomic interactions between the nicotinamide ring and its binding pocket residues in the 3 α -HSD•NADP⁺•testosterone complex (27).

Members of the AKR superfamily, such as human aldose reductase, aldehyde reductase, 3 α -HSD, 17 β -HSD, and 20 α -HSD, share more than 45% amino acid sequence identity (12–16). Most AKRs exhibit specificity toward NADP(H), whereas 3 α -HSD displays dual pyridine nucleotide specificity and is able to use either NADP(H) or NAD(H) for the oxidoreduction of steroids. The amino acid residues that bind the nicotinamide cofactor are virtually identical in all known AKRs (5). In the 3 α -HSD•NADP⁺ binary complex structure, there are 14 residues that directly contact NADP⁺ (7). The nicotinamide ring (or headgroup) forms a π -stacking interaction with the side chain of Tyr 216 at the core of the barrel and is oriented to maintain its stereochemistry by a network of three hydrogen bonds between the C3-carboxamide group and the side chains of Ser 166, Asn 167, and Gln 190 (Figure 1 shows the interactions in the 3 α -HSD•NADP⁺•testosterone complex). These interactions permit 4-*pro-R* hydride transfer from the A-face of the pyridine nucleotide cofactor to the β -face of the steroid substrate, and as a result the *anti*-antiperiplanar 1,4-dihydronicotinamide ring in NADPH is oxidized to the planar form. The 2'-phosphate group on the AMP moiety (or tail group) of NADP⁺ forms a hydrogen bond and a salt bridge with Ser 271 and Arg 276, respectively (7). Mutagenesis studies with other AKRs have examined the roles of amino acids that contact the 2'-AMP moiety (17–19) and indicate that the salt bridge that forms between the enzyme and the 2'-phosphate of the AMP moiety is a major reason most AKRs prefer NADP(H) over NAD(H). However, no systematic studies have been performed to elucidate the roles of the residues that bind the nicotinamide ring (headgroup) of the dinucleotide in either AKRs or SDRs.

In this work, we used site-directed mutagenesis to investigate the roles of Ser 166, Asn 167, Gln 190, and Tyr 216 which are thought to be important in binding the nicotinamide ring of the cofactor, based on the crystal structure of the 3 α -HSD•NADP⁺ complex (7). The effect of mutating these residues on dissociation constants and steady-state kinetic parameters was different for NADP(H) as compared to that for NAD(H). Changes in the binding energies on mutating

these residues suggested that they contributed toward binding NADP(H) in both the ground state and the transition state. However, the same residues contributed toward binding NAD(H) in the transition state only. These findings suggest that different binding modes exist for NADP(H) and NAD(H) and that these modes are revealed by mutating residues that surround the nicotinamide (headgroup) as opposed to the 2'-AMP (tail group). These point mutations were insufficient to either invert or racemize the stereochemistry of hydride transfer even though the nicotinamide pocket can accommodate both *anti*- and *syn*-conformations once the hydrogen bonds are eliminated. However, stereospecific transfer of the 4-*pro-R* tritide was reduced reflecting a pronounced primary kinetic isotope effect. This isotope effect and the change in transition-state binding energy for NAD(P)(H) observed in the mutants suggest that the reaction trajectory has been altered.

EXPERIMENTAL PROCEDURES

Materials. The primers used for PCR-based site-directed mutagenesis were synthesized by Gibco BRL. Goat anti-rabbit IgG-horseradish peroxidase conjugate and 4-chloro-1-naphthol were purchased from BioRad. The polyclonal rabbit anti-rat 3 α -HSD antiserum has been described (20). NAD(H) and NADP(H) were purchased from Boehringer-Mannheim. Deuterated ethanol (ethanol-*d*₆, 99% D atom excess) was purchased from Cambridge Isotope Laboratories. All unradio-labeled steroids were obtained from Steraloids. Radiolabeled [4-³H]NAD⁺ (250 μ Ci/mmol) was purchased from Amersham Pharmacia Biotech. [¹⁴C]-5 α -DHT (50 mCi/mmol) was obtained from NEN DuPont. Whatman DE-52 was from Baxter; Sepharose-Blue, Sephadex G100, Polybuffer 74, and PBE 94 were purchased from Pharmacia Biotech. Centriplus 10 concentrators were from Amicon, Inc. Yeast alcohol dehydrogenase (430 units/mg), 3/17 β -HSD (35 unit/mg) from *P. testosteroni*, D-glyceraldehyde-3-phosphate dehydrogenase (120 units/mg) from rabbit muscle, and yeast 3-phosphoglyceric phosphokinase (1600 units/mg) were obtained from Sigma-Aldrich. NADP⁺ specific alcohol dehydrogenase from *L. mesenteroides* was purchased from Research Plus, Inc. All other compounds were ACS grade or better.

Mutagenesis, Expression, and Purification of Recombinant Wild-Type and Mutant 3 α -HSDs. The pKK-3 α -HSD expression vector and details of the PCR-based site-directed mutagenesis protocols have been previously described (21). The forward and reverse primers used to produce the S166A, N167A, Q190A, and Y216S mutants are listed below, respectively: 5'-dCTATTGGGGTGGCCAACTTTAACTG-3', 5'-dCAGTTAAAGTTGGCCACCCCAATAG-3'; 5'-dT-TGGGGTGTCCGCCTTTAACTGCAG-3', 5'-dCTGCAGTT-AAAGGCGGACACCCCA-3'; 5'-TGTGTGCAACGCA-GTGGAATGTCA-3', 5'-dTGACATTCCACTGCGTTGCA-CACA-3'; 5'-dTTCGTGGTTTCCTCCTGCACGCTGGG-3', 5'-dCCCAGCGTGCAGGAGGAAACCAGAA-3'. The underlined bases indicate the mutated codons. The flanking forward and reverse primers were 5'-dCCGGCTCGTATAAT-GTGTGGA-3' and 5'-dCAGACCGCTTCTGCGTTCT-3'. The mutants were generated by two rounds of PCR (21, 22). The first round of PCR used the mutated primers and the flanking primers to generate the fragment containing the point mutations at either the 5' or 3' end. Then the second round

of PCR was used to amplify the mutants with the flanking primers after annealing the first-round PCR products together. The final PCR products were ligated into the pKK-3 α -HSD expression vector lacking the mutated fragment. Dideoxy-sequencing ensured fidelity of the mutant constructs. The mutant expression vectors were used to transform competent *E. coli* DH5 α cells, and the overexpressed proteins were purified as described (22) with the exception of the N167A mutant.

The N167A mutant was purified via a similar protocol, except chromatofocusing (PBE 94) and gel filtration (G-100) chromatography steps were introduced between the DE-52 cellulose column and Sepharose-Blue column to remove contaminating proteins. In this method, proteins eluted from the DE-52 column were dialyzed overnight in buffer A (25 mM imidazole/HCl buffer, pH 7.4, containing 1 mM EDTA, 1 mM β -mercaptoethanol, 20% glycerol) and then loaded onto the PBE 94 column. After equilibration with 10–15 bed volumes of buffer A, the protein was eluted with buffer B (mixture of 1 volume of Polybuffer 74/HCl, pH 5.0, with 8 volumes of 20% glycerol containing 1 mM EDTA, 1 mM β -mercaptoethanol). Purity of the eluted protein was checked by SDS–PAGE, and the desired fractions were collected and dialyzed overnight in buffer C (25 mM potassium phosphate buffer, pH 7.0, containing 1 mM EDTA, 1 mM β -mercaptoethanol, 20% glycerol). Protein was then loaded on a Sephadex G100 column and eluted with buffer C. The protein was concentrated using the Centrplus 10 concentrators, dialyzed overnight against buffer D (10 mM potassium phosphate buffer, pH 7.0, containing 1 mM EDTA, 1 mM β -mercaptoethanol, 20% glycerol), and further purified by Sepharose-Blue chromatography.

SDS–PAGE was used to assess final protein purity, and protein concentration was determined by the method of Lowry (23). Immunoblots confirmed the identity of all expressed proteins using a 1:1000 dilution of the polyclonal rabbit anti-rat 3 α -HSD sera 71535 (24). Homogeneous mutant enzymes were stored at -80°C . Enzyme activity was monitored using a standard assay system containing 100 mM potassium phosphate buffer, pH 7.0, 2.3 mM NAD(P) $^{+}$, and 75 μM androsterone with 4% acetonitrile as cosolvent.

Determination of K_d Values for NAD(H) and NADP(H) by Fluorescence Titration. K_d values for the binding of cofactors to recombinant wild-type and the mutant enzymes were determined by measuring protein fluorescence on a Perkin-Elmer 650-10S spectrofluorometer following the incremental addition of NAD(H) (35–300 μM) and NADP(H) (80 nM–4.0 μM). Each 1-mL sample contained 0.5 μM protein in 10 or 100 mM potassium phosphate, pH 7.0 [NAD(P) $^{+}$] or pH 6.0 [NAD(P)H] buffer at 25°C . The total volume change from addition of cofactors was less than 2%. The samples were excited at 290 nm with fluorescence emission scanned from 300 to 500 nm at 120 nm/min with excitation and emission band-pass each set at 5 nm. Untransformed fluorescence data were plotted as percent change in fluorescence at emission λ_{max} (% ΔF) versus cofactor concentration. Fitting of these data to a saturation absorption isotherm by ENZFITTER provided an estimate of the K_d and the associated standard errors (25).

Steady-State Enzyme Kinetics. Initial velocities were measured in a Beckman DU-640 spectrophotometer by

observing the rate of change in absorbance of pyridine nucleotide at 340 nm ($\epsilon = 6270 \text{ M}^{-1} \text{ cm}^{-1}$) in 1-mL systems at 25°C using a 1-cm path length cuvette. The steady-state kinetic parameters for androsterone oxidation were determined with varied steroid concentration (1.5–75.0 μM androsterone at 2.3 mM NAD(P) $^{+}$) and for androstanedione reduction with varied steroid concentration (0.3–35 μM androstanedione at 180 μM NAD(P)H). The kinetic parameters for NAD(P) $^{+}$ reduction were determined at 75 μM androsterone by varying the NAD(P) $^{+}$ concentrations (170–2300 μM NAD $^{+}$ and 2.0–2300 μM NADP $^{+}$) and for NAD(P)H oxidation at 35 μM androstanedione with varying NAD(P)H concentrations (3.5–180 μM NADH and 0.5–180 μM NADPH). Oxidation reactions were performed in 100 mM potassium phosphate buffer, pH 7.0, and the reduction reactions were performed in 100 mM potassium phosphate buffer, pH 6.0. All reactions were initiated by the addition of enzyme. Calculation of k_{cat} and K_m values used the ENZFITTER nonlinear regression analysis program to fit untransformed data with a hyperbolic function, as originally described by Wilkinson (26), yielding estimates of the kinetic constants and the associated standard errors.

Molecular Modeling Studies to Accommodate the *syn*-Conformation of NADP $^{+}$. Molecular modeling studies were performed on a Silicon Graphics Indy workstation by utilizing the program QUANTA (Molecular Simulations, Inc.). The rat liver 3 α -HSD·NADP $^{+}$ ·testosterone complex was used as the starting structure (1AFS, PDB file) (27). In this structure, the nicotinamide ring is in an *anti*-conformation so that the A-face of the ring lies toward the β -face of the steroid to permit 4-*pro-R* hydride transfer (Figure 1). To determine whether the structure could accommodate the nicotinamide ring in the *syn*-conformation and permit 4-*pro-S* hydride transfer, the hydrogen bonds between the carboxamide group and residues Ser 166, Asn 167, and Gln 190 were eliminated and the nicotinamide ring with the *syn*-conformation was docked into the site.

Synthesis of 4-*pro-R*- and 4-*pro-S*-[^3H]NADH. The stereospecifically labeled 4-*pro-R*- and 4-*pro-S*-[^3H]NADH were synthesized enzymically from [4- ^3H]NAD $^{+}$ by the method of Leowus et al. (28,29) and Askonas et al. (9) with minor modifications. The 4-*pro-S*-[^3H]NADH was synthesized using yeast alcohol dehydrogenase to catalyze the stereospecific oxidation of ethanol using [4- ^3H]NAD $^{+}$ as cofactor. The system contained 20 mM sodium pyrophosphate buffer, pH 10.0, 2% (v/v) ethanol, 180 μM unlabeled NAD $^{+}$, and 0.5 μM [4- ^3H]NAD $^{+}$ (2 $\mu\text{Ci/nMol}$), and the reaction was initiated by adding yeast alcohol dehydrogenase. The reaction mixture was then lyophilized. The 4-*pro-R*-[^3H]NADH was synthesized using glyceraldehyde-3-phosphate dehydrogenase to catalyze the stereospecific oxidation of glyceraldehyde-3-phosphate using [4- ^3H]NAD $^{+}$ as cofactor. The system contained 100 mM Tris/HCl buffer, pH 8.0, freshly hydrolyzed DL-glyceraldehyde-3-phosphate diethyl acetal (7.3 mM), 1 mM adenosine-5'-diphosphate (ADP), 3.3 mM cysteine/HCl, 20 mM K $_2$ HPO $_4$, 2% (v/v) acetonitrile, 330 μM unlabeled NAD $^{+}$, and 0.5 μM [4- ^3H]NAD $^{+}$, and the reaction was initiated by adding both 3-phosphoglyceric phosphokinase and glyceraldehyde-3-phosphate dehydrogenase. The final product was loaded on a DE-52 cellulose column, equilibrated with 10 mM Tris/HCl buffer, pH 8.0, and then eluted with the same buffer containing 50 mM

NaCl. The fractions with the highest absorbance at 340 nm and tritium radioactivity were pooled and lyophilized. The final product was redissolved in 10 mM potassium phosphate buffer, pH 6.0. In each case the specific radioactivity was calculated by measuring the absorbance at 340 nm using $\epsilon = 6270 \text{ M}^{-1}\text{cm}^{-1}$ and by counting an aliquot of the radiolabeled cofactor.

Stereospecificity of Hydride Transfer. The stereospecificity of hydride transfer catalyzed by the mutant enzymes was determined using stereospecifically radiolabeled cofactors as hydride donors and [^{14}C]-5 α -DHT as the hydride acceptor. A 3-mL reaction system was used with 75 μM [^{14}C]-5 α -DHT ($3.5 \times 10^3 \text{ cpm/nmol}$) as substrate and 180 μM [^3H]-NADH ($1\text{--}1.8 \times 10^4 \text{ cpm/nmol}$) as cofactor. The reaction was initiated by addition of either the wild-type or mutant enzyme and was quenched when no more absorbance change was observed. The steroid product was extracted with water-saturated ethyl acetate ($3 \times 2 \text{ mL}$), vacuum-dried, and redissolved in 0.1 mL of methanol. The radioactive steroid was applied to 20- \times 20-cm thin layer chromatography plates (Whatman Inc.) and developed in toluene:ethyl acetate (3:1, v:v) (30). Wild-type 3 α -HSD was used as a positive control for 4-*pro-R* hydride transfer and the 3/17 β -hydroxysteroid dehydrogenase from *P. testosteronei* was used as positive control for 4-*pro-S* hydride transfer.

Synthesis and Purification of 4-*pro-R*-NADPD. 4-*pro-R*-NADPD was synthesized by the method of Viola et al. (31) with the following modifications. The reaction was performed in 10 mM sodium pyrophosphate, pH 10.0 at 25 $^{\circ}\text{C}$, with excess deuterated ethanol and 1 mM NADP^+ as cofactor, using NADP^+ -specific *L. mesenteroides* alcohol dehydrogenase. The reaction was followed to completion by monitoring the change in absorbance at 340 nm. The reaction mixture was then subjected to anion-exchange chromatography on a Whatman DE-52 column, equilibrated in 50 mM Tris-HCl, pH 8.0, and eluted using a gradient of 50 mM Tris-HCl, pH 8.0, to 500 mM Tris-HCl, pH 8.0. The purity of the eluted NADPD was determined on the basis of A_{260}/A_{340} (2.3 or less), and the concentration was calculated using A_{340} , with $\epsilon_{340} = 6270 \text{ M}^{-1} \text{ cm}^{-1}$.

RESULTS

Expression and Purification of Recombinant Wild-Type and Mutant 3 α -HSDs. Wild-type 3 α -HSD and the S166A, N167A, Q190A, and Y216S mutants were overexpressed in *E. coli* DH5 α cells and purified to homogeneity (Table 1). The mutant enzymes gave single bands of $\sim 37 \text{ kDa}$ on SDS-PAGE, which were immunoreactive with rabbit anti-rat 3 α -HSD antiserum upon Western blot analysis. The specific activities for androsterone oxidation were 1.55, 0.096, and 0.080 $\mu\text{mol/min/mg}$ for recombinant wild-type enzyme, S166A, and Q190A, respectively, with NAD^+ as cofactor. The specific activity of Y216S was 0.81 $\mu\text{mol/min/mg}$ with NADP^+ as cofactor. NADP^+ was used in this case, as the activity of Y216S was undetectable with NAD^+ . All proteins were obtained in high yield except the N167A mutant, which was expressed poorly and could not be purified without the additional steps of chromatofocusing and gel filtration chromatography. Purified N167A was obtained in low yield, and three preparations gave a total of 3.5 mg of protein; the catalytic activity of this mutant toward steroid

Table 1: Purification of Recombinant 3 α -HSD and Its Nicotinamide Pocket Mutants^a

	total vol (mL)	total activity ($\mu\text{mol/min}$)	total prot (mg)	specific activity ($\mu\text{mol/min/mg}$)	purifn factor	yield (%)
Recombinant wt 3 α -HSD						
sonicate	63	156.3	1282.7	0.12	1	100
DE-52	14	54.5	84.4	0.65	5.3	34.9
cellulose						
Blue-Sephacrose	7.5	49.6	32.1	1.55	12.7	31.7
S166A						
sonicate	55	7.3	1432.6	0.005	1	100
DE-52	17	3.5	104.9	0.03	6.6	47.8
cellulose						
Blue-Sephacrose	4.8	3.1	32.5	0.10	18.9	42.8
Q190A						
sonicate	68	4.9	1869.0	0.003	1	100
DE-52	15	4.1	108.8	0.04	14.2	82.4
cellulose						
Blue-Sephacrose	6.0	3.3	40.6	0.08	30.3	65.9
Y216S						
sonicate	60	47.1	1537.8	0.03	1	100
DE-52	14	33.2	71.3	0.47	15.2	70.4
cellulose						
Blue-Sephacrose	6.1	30.6	37.9	0.81	26.4	65.1

^a Activity measurements were performed under standard assay conditions of 100 mM potassium phosphate, pH 7.0, containing either 2.3 mM NAD^+ (wild-type, S166A, and Q190A) or 2.3 mM NADP^+ (Y216S), 75 μM androsterone, and 4% acetonitrile at 25 $^{\circ}\text{C}$.

was extremely poor and could only be detected by using a radiometric assay with [^{14}C]-5 α -DHT as substrate (data not shown).

Determination of Dissociation Constants for Cofactors in the Mutants. 3 α -HSD displays an ordered kinetic mechanism in which pyridine nucleotide binds first and leaves last (9). As a result the formation of the binary complexes, $\text{E}\cdot\text{NAD(P)H}$ and $\text{E}\cdot\text{NAD(P)}^+$, can be measured by titrating the intrinsic protein fluorescence upon the incremental addition of cofactor. To compare the K_d values obtained for the wild-type and mutant enzymes directly with steady-state kinetic parameters, all measurements were performed in the same buffer used for steady-state kinetics (Table 2). Under these conditions the S166A, Q190A, and Y216S mutants exhibited a 2–10-fold increase in the K_d^{NADPH} and a 4–11-fold increase in the $K_d^{\text{NADP}^+}$ versus wild-type enzyme. With both cofactors, Y216S mutant exhibited the largest increase in K_d . Surprisingly, the $K_d^{\text{NAD(H)}}$ was unchanged in these mutants.

Steady-State Kinetic Properties of the Mutants. Steady-state kinetic properties of the recombinant enzyme and the three mutants S166A, Q190A, and Y216S were compared using NAD(P)^+ as the cofactor and androsterone as substrate in the oxidation direction and NAD(P)H as the cofactor and androstenedione as the substrate in the reduction direction (Table 3). N167A exhibited no detectable rate in either direction under the conditions of this spectrophotometric assay. The remaining mutants had profound effects on the steady-state kinetic parameters, and the most pronounced effects were seen when NAD(H) was used.

$K_m^{\text{NADP}^+}$ increased 13–151-fold in the mutants, and this change was reflected by a comparable decrease in $k_{\text{cat}}/K_m^{\text{NADP}^+}$. The similar changes in K_m and k_{cat}/K_m observed in these mutants suggest that their predominant effect is on

Table 2: K_d Values of Cofactors for 3 α -HSD and Its Mutants Determined by Fluorescence Titration

nucleotide	recombinant wt 3 α -HSD ^a (μ M)	recombinant wt 3 α -HSD (μ M)	S166A (μ M)	S166A/wt	Q190A (μ M)	Q190A/wt	Y216S (μ M)	Y216S/wt
NADPH	0.2 \pm 0.01	0.4 \pm 0.02	1.0 \pm 0.1	2.3	1.5 \pm 0.1	3.6	4.2 \pm 0.5	10.0
NADP ⁺	0.4 \pm 0.01	0.9 \pm 0.1	3.6 \pm 0.1	4.2	7.0 \pm 1.6	8.2	9.3 \pm 3.3	10.9
NADH	182 \pm 28	120 \pm 7	104 \pm 5	0.9	107 \pm 5	0.9	139 \pm 9	1.2
NAD ⁺	212 \pm 25	174 \pm 17	124 \pm 13	0.7	171 \pm 10	1.0	131 \pm 3	0.8

^a All fluorescence titration measurements were performed in 100 mM potassium phosphate, pH 7.0, except column 1 which was performed in 10 mM potassium phosphate, pH 7.0, and these values were in accord with those previously reported (22).

Table 3: Kinetic Comparison of Nicotinamide Pocket Mutants Using NADP(H) as Cofactor^a

substrate	recombinant wt 3 α -HSD	S166A/wt	Q190A/wt	Y216S/wt
androsterone				
k_{cat} (min^{-1})	39.0 \pm 1.2	2.4	3.8	2.0
K_m (μ M)	4.1 \pm 0.5	4.2	8.7	24.1
k_{cat}/K_m ($\text{min}^{-1} \mu\text{M}^{-1}$)	9.5	0.6	0.4	0.08
NADP ⁺				
k_{cat} (min^{-1})	43.7 \pm 0.1	1.6	2.1	1.08
K_m (μ M)	5.2 \pm 0.6	13.3	40.6	151.5
k_{cat}/K_m ($\text{min}^{-1} \mu\text{M}^{-1}$)	8.4	0.1	0.05	0.01
androstenedione				
k_{cat} (min^{-1})	33.5 \pm 3.7	1.2	0.6	0.06
K_m (μ M)	3.9 \pm 0.6	1.1	1.6	1.1
k_{cat}/K_m ($\text{min}^{-1} \mu\text{M}^{-1}$)	8.6	1.2	0.4	0.05
NADPH				
k_{cat} (min^{-1})	47.3 \pm 5.5	0.8	0.6	0.04
K_m (μ M)	2.2 \pm 0.8	2.2	8.1	4.9
k_{cat}/K_m ($\text{min}^{-1} \mu\text{M}^{-1}$)	21.5	0.4	0.1	0.01

^a All activity measurements were performed in a 1-mL system at 25 $^{\circ}\text{C}$, and rates were determined by measuring the change in absorbance of pyridine nucleotide at 340 nm; see details under Experimental Procedures. ND, not detectable.

cofactor K_m (Table 3). The effects on the kinetic parameters for androsterone were less dramatic: the K_m of androsterone increased 4–24-fold and the k_{cat} increased 2–4-fold resulting in catalytic efficiencies that were decreased by only 2–12-fold. In the reduction direction, the mutants displayed minimal effects on the K_m and k_{cat} values for NADPH and androstenedione, the exception being the Y216S mutant for which $k_{\text{cat}}^{\text{NADPH}}$ decreased by 17-fold.

By contrast, $K_m^{\text{NAD}^+}$ only increased 4–8-fold, but k_{cat} values decreased 4–103-fold, resulting in changes in catalytic efficiency of 23–930-fold (Table 4). Thus the predominant effect of these mutants is on k_{cat} . For the substrate androsterone, the effects on K_m values were relatively modest and the decreases in k_{cat}/K_m were primarily due to the decreases in k_{cat} . In the reduction direction $k_{\text{cat}}^{\text{NADH}}$ and $k_{\text{cat}}^{\text{androstenedione}}$ decreased by 2–14-fold for the S166A and Q190A mutants and K_m^{NADH} and $K_m^{\text{androstenedione}}$ increased by similar amounts.

Changes in Cofactor Binding Energy in the Mutants. We also investigated the role of these mutants in disrupting the binding interactions between the enzyme and cofactor (32, 33) (Table 5). The contribution to ground-state binding energy was determined by the equation: $\Delta\Delta G_b = -RT \ln[(K_d)_{\text{wt}}/(K_d)_{\text{mut}}]$. The contribution to transition-state binding energy was calculated from the equation: $\Delta\Delta G_b^{\ddagger} = RT \ln[(k_{\text{cat}}/K_m)_{\text{wt}}/(k_{\text{cat}}/K_m)_{\text{mut}}]$. We found that the wild-type 3 α -HSD contributes 3.1 kcal/mol more toward binding NADP(H) as compared to NAD(H), most of which are likely due to the electrostatic link between Arg 276 and the 2'-phosphate group on the AMP moiety of NADP(H) (34). These $\Delta\Delta G_b$ values are also similar to those obtained for human aldose reductase (21) and human dihydrodiol dehydrogenase 4

Table 4: Kinetic Comparison of Nicotinamide Pocket Mutants Using NAD(H) as Cofactor^a

substrate	recombinant wt 3 α -HSD	S166A/wt	Q190A/wt	Y216S/wt
androsterone				
k_{cat} (min^{-1})	98.1 \pm 8.5	0.2	0.2	0.01
K_m (μ M)	44.1 \pm 7.8	1.3	3.5	8.7
k_{cat}/K_m ($\text{min}^{-1} \mu\text{M}^{-1}$)	2.2	0.1	0.05	0.001
NAD ⁺				
k_{cat} (min^{-1})	76.4 \pm 4.1	0.2	0.2	0.01
K_m (μ M)	821 \pm 124	5.6	4.0	7.9
k_{cat}/K_m ($\text{min}^{-1} \mu\text{M}^{-1}$)	0.09	0.04	0.03	0.001
androstenedione				
k_{cat} (min^{-1})	18.6 \pm 0.2	0.5	0.2	ND
K_m (μ M)	3.9 \pm 0.6	15.2	30.4	ND
k_{cat}/K_m ($\text{min}^{-1} \mu\text{M}^{-1}$)	4.8	0.03	0.01	ND
NADH				
k_{cat} (min^{-1})	23.3 \pm 1.5	0.2	0.1	ND
K_m (μ M)	31.2 \pm 4.6	5.7	10.7	ND
k_{cat}/K_m ($\text{min}^{-1} \mu\text{M}^{-1}$)	0.7	0.04	0.01	ND

^a All activity measurements were performed in a 1-mL system at 25 $^{\circ}\text{C}$, and rates were determined by measuring the change in absorbance of pyridine nucleotide at 340 nm; see details under Experimental Procedures. ND, not detectable.

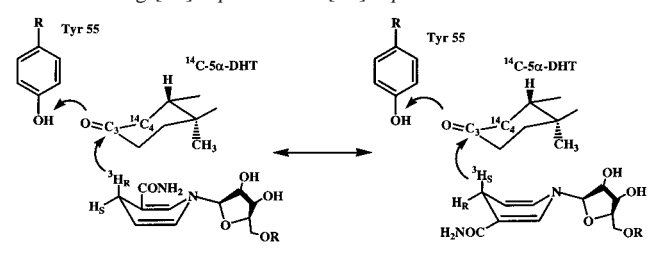
(DD4) (19) and support the observation that these enzymes bind NADP(H) tighter than NAD(H). When NADPH was used as cofactor, mutations of Ser 166, Gln 190, and Tyr 216 led to a loss of 0.5–1.3 kcal/mol in ground-state binding energy and 0.6–2.7 kcal/mol in transition-state binding energy. When NADP⁺ was used as cofactor, these mutations led to a loss of 0.8–1.4 kcal/mol in ground-state binding energy and 1.2–2.9 kcal/mol in transition-state binding energy. These data indicated that of the three residues, Tyr 216 contributed the greatest to the cofactor binding energy in both the ground and transition states. When NAD(H) was used as cofactor, the contributions toward the ground-state binding energy from Ser 166, Gln 190, and Tyr 216 were minimal. However, all three residues contributed significantly toward the transition-state binding energy, with changes in energy varying from 1.8 to 4.0 kcal/mol.

Examination of the Stereospecificity of Hydride Transfer in the Mutants. In 3 α -HSD, the nicotinamide ring adopts an *anti*-conformation with respect to the ribose ring. This conformation is dictated by hydrogen bonds formed between the enzyme and the C3-carboxamide group. Modeling studies indicated that if the hydrogen bonds were eliminated a *syn*-conformation could also be accommodated at the active site. To examine the roles of the mutated residues in maintaining the stereochemistry of hydride transfer, we synthesized stereospecifically labeled 4-*pro-R*-[³H]NADH and 4-*pro-S*-[³H]NADH and used them as hydride donors for the reduction of [¹⁴C]-5 α -DHT (Table 6). When 4-*pro-R*-[³H]-NADH was used as the hydride donor, the ³H:¹⁴C ratio was 4.1 for wild-type 3 α -HSD and decreased by 50% in the mutants suggesting that a decrease in the incorporation of

Table 5: Effects of Mutants on Cofactor Binding Energy in 3 α -HSD^a

modification	rwt 3 α -HSD \rightarrow S166A		rwt 3 α -HSD \rightarrow Q190A		rwt 3 α -HSD \rightarrow Y216S	
	$\Delta\Delta G_b$ (kcal/mol)	$\Delta\Delta G_b^\ddagger$ (kcal/mol)	$\Delta\Delta G_b$ (kcal/mol)	$\Delta\Delta G_b^\ddagger$ (kcal/mol)	$\Delta\Delta G_b$ (kcal/mol)	$\Delta\Delta G_b^\ddagger$ (kcal/mol)
NADPH	0.5	0.6	0.8	1.5	1.3	2.7
NADP ⁺	0.8	1.2	1.3	1.8	1.4	2.9
NADH	-0.1	1.9	-0.1	2.9	0.1	—
NAD ⁺	-0.2	1.8	-0.01	2.0	-0.2	4.0

^a rwt 3 α -HSD, recombinant wt 3 α -HSD; $\Delta\Delta G_b = -RT \ln[(K_d)_{wt}/(K_d)_{mut}]$ and $\Delta\Delta G_b^\ddagger = RT \ln[(k_{cat}/K_m)_{wt}/(k_{cat}/K_m)_{mut}]$, where R is the gas constant and T is temperature in Kelvins.

Table 6: Stereochemistry of Hydride Transfer Catalyzed by the Mutants Using [³H]-4-*pro-R*- and [³H]-4-*pro-S*-NADH


		Anti-antiperiplanar					Syn-antiperiplanar		
reactions	ratio ^a	wt	recombinant	S166A	Q190A	Y216S			
4- <i>pro-R</i> -[³ H]NADH	³ H: ¹⁴ C	ND	4.1	2.4	2.3	1.9			
4- <i>pro-S</i> -[³ H]NADH	³ H: ¹⁴ C	12.4	0.6	0.6	0.4	0.3			

^a³H:¹⁴C ratio in steroid product at the completion of the reactions.

4-*pro-R* tritium had occurred. When 4-*pro-S*-[³H]NADH was used as hydride donor, the ³H:¹⁴C ratio was 12.4 in the positive control (3/17 β -HSD reactions) and 0.6 in the negative control (3 α -HSD reactions) confirming that the incorporation of the 4-*pro-R* hydrogen is more than 95% stereoselective. Previous studies have estimated *re*-face hydride transfer to be better than 98% stereoselective in A-face specific dehydrogenases (28). When the mutants were substituted, the ³H:¹⁴C ratios did not increase above the negative control, which suggests that there was no increase in the incorporation of the 4-*pro-S* hydrogen into [¹⁴C]-5 α -DHT in the mutants. Thus the decrease in the ³H:¹⁴C ratio catalyzed by the mutants is not a reflection of an inversion of stereochemistry but more likely reflects a primary kinetic isotope effect on hydride transfer. This hypothesis was supported by determining the primary kinetic isotope effect in wild-type 3 α -HSD and the mutant Q190A using 4-*pro-R*-NADPD, in which the ^D k_{cat}/K_m of wild-type 3 α -HSD was 0.8 for androstenedione but was 1.6 in mutant Q190A (35). For an ordered bi-bi reaction, k_{cat}/K_m reflects the binding and release of the second substrate and the chemical step (36).

DISCUSSION

In this paper, we report the first systematic studies examining the role of conserved residues in AKRs that are involved in binding the nicotinamide ring (headgroup) of the dinucleotide NAD(P)(H). Our data show that these residues contribute to the high-affinity binding for NADP(H) but do not influence the binding of NAD(H), whereas the reaction trajectory with both cofactors is defined by these residues.

Nicotinamide Binding Residues Play Important Roles in Cofactor Binding. The crystal structure of the 3 α -HSD

NADP⁺•testosterone complex indicates that the aromatic ring of Tyr 216 is involved in a π -stacking interaction with the nicotinamide ring. The formation of three hydrogen bonds between Ser 166, Asn 167, and Gln 190 with the C3-carboxamide substituent of the pyridine ring of NADP⁺ maintains the *anti*-conformation necessary for the stereospecific transfer of the 4-*pro-R* hydrogen to the 3-ketosteroid (7). Our site-directed mutagenesis studies on these residues showed that they played an important role in binding NADP(H) but not NAD(H) in the ground state.

Mutation of Asn 167 resulted in the most impaired enzyme, and its catalytic activity could only be detected by a radiometric assay. The remaining mutant enzymes (Y216S, Q190A, and S166A) exhibited decreased binding affinity for NADP(H) by 2–11-fold (Table 2). The changes in binding energy were consistent with the role of Tyr 216 in π -stacking and the contribution of hydrogen bonds from the remaining two residues (Table 5). The increases in K_d observed were also reflected in the steady-state kinetic parameters for NADP⁺. These mutations led to corresponding increases in $K_m^{NADP^+}$, and the decrease in k_{cat}/K_m could be explained predominantly by the change in K_m . Significantly, the impact on $K_m^{NADP^+}$ was much larger than on K_m^{NADPH} . This difference may arise due to the fact that the nicotinamide ring of NADP⁺ is more planar than that of NADPH and the binding pocket may prefer to accommodate this conformation over the boat-shaped conformation of the reduced cofactor. These mutants did not affect K_d values of NAD(H), and changes in $K_m^{NAD(H)}$ were small. However, the effect on k_{cat}/K_m was dramatic, indicating that the chemical step was affected in each mutant. Our findings suggest that these residues are important for maintaining transition-state binding energy.

Differences in the Binding Modes of NADP(H) and NAD(H). Several observations suggest that the binding modes for NADP(H) and NAD(H) are different. First, mutations in the Ser 166, Gln 190, and Tyr 216, residues known to have important interactions with NADP(H), have no effect on $K_d^{NAD(H)}$ (Table 2). Second, changes in the steady-state kinetic parameters indicate that while these mutations predominantly affect $K_m^{NADP^+}$, the effect is less dramatic on $K_m^{NAD^+}$, while profound effects were observed in $k_{cat}/K_m^{NAD^+}$ (Tables 3 and 4). The effect on catalytic efficiency is likely to reflect changes in the chemical step. This is borne out by a calculation of the change in free energies associated with the binding of NAD(P)(H) in the ground and transition states in the various mutants. These results show that while the binding of NADP(H) is adversely affected in both the ground and transition states, the binding of NAD(H) is adversely affected only in the transition state. Thus these mutants only affect the binding of cofactor in the actual bond-breaking and bond-forming events. This would suggest that the binding

of NAD(H) to 3 α -HSD in the ground state is different from that of NADP(H) (Table 5). Third, previous fluorescence stopped-flow studies have shown that while the binding of NADPH is explained by a two-step model in which a loose complex, E•NADP(H), isomerizes to a tight complex, E•*NADP(H), measured as a fluorescence kinetic transient, no such transient was observed with NAD(H) (34). Further, that work showed that the kinetic transient had an obligatory requirement for the formation of an electrostatic linkage between Arg 276 and the 2'-phosphate group of NADPH. This interaction is not possible with NAD(H) (34). These data together provide compelling evidence for two modes of cofactor binding with 3 α -HSD and that the head residues contribute to these differences.

Influence of Nicotinamide Pocket Mutants on k_{cat} . 3 α -HSD has an ordered bi-bi kinetic mechanism (9), and for such a mechanism, k_{cat} reflects all steps on the reaction coordinate (37). Studies on recombinant human placental aldose reductase showed that the movement of loop B (the nucleotide clamping loop) is the overall rate-limiting step, and stopped-flow studies indicated that the E•*NADP(H) \rightarrow E•NADP(H) isomerization event, prior to release of cofactor, was the slowest step (38). However, similar stopped-flow studies in 3 α -HSD showed that all events associated with cofactor binding and release are much faster than k_{cat} and that the E•*NADP(H) \leftrightarrow E•NADP(H) event is not the rate-limiting step overall for this enzyme. Since the binding and release of steroid is faster than the binding and release of cofactor, the chemical step would appear to be rate-limiting overall (9). Kinetic studies on nicotinamide pocket mutants indicated that mutations altered the values of k_{cat} for NADP(H) and NAD(H), suggesting that the chemical step in these enzymes had been affected. Since all these residues are located at the catalytic center, it is not surprising that mutating them will affect the conformation of the cofactor and likely alter the optimal reaction trajectory (39, 40).

Factors Influencing the Stereochemistry of Hydride Transfer. SDRs and AKRs exhibit opposite stereospecificity of hydride transfer. The question arises as to how two different enzyme superfamilies evolved to catalyze the same chemical reaction with the same cofactor, but with opposite stereochemistries. In 3 α -HSD, the *anti*-conformation adopted by the nicotinamide ring is dictated by residues in the binding pocket. Models of the 3 α -HSD ternary complex structure predict that the pocket could accommodate a *syn*-conformation if the hydrogen bonds provided by Ser 166, Asn 167, and Gln 190 were eliminated (Figure 1). However, there are some caveats concerning the model in which the *syn*-conformation of cofactor is bound. First, there is no residue within optimal distance of the carboxamide group to stabilize the *syn*-conformation with hydrogen bonds. These interactions are a major force in stabilizing the *anti*-conformation of the nicotinamide ring in 3 α -HSD. Second, the substrate binding residue Trp 227 is within van der Waals radius of the flipped carboxamide group and possibly causes steric hindrance in binding the *syn*-conformation. We examined S166A, Q190A, and Y216S to determine if mutating these residues individually resulted in the stereospecificity of the reaction being inverted or racemized (Table 6). To evaluate these mutants we followed the incorporation of [3 H]-4-*pro-R* and [3 H]-4-*pro-S* hydrogens from NADH into [14 C]-5 α -DHT and scored the 3 H: 14 C ratios. Our data showed that

while the mutants decreased the 3 H: 14 C ratio with the 4-*pro-R*-labeled cofactors, there was no concomitant increase in the 3 H: 14 C ratio with the 4-*pro-S*-labeled cofactors. The likely explanation is that the decrease in the 3 H: 14 C ratio reflects a primary isotope effect in the reactions catalyzed by these mutants. This was examined by measurement of $^Dk_{cat}/K_m$ for wild-type enzyme (0.8) and measurement of $^Dk_{cat}/K_m$ for Q190A mutant (1.6) using 4-*pro-R*-NADPD (35). Although these data were generated with NADPD and the stereochemistry of hydride transfer was defined with NADH, the comparison is valid since we have shown that the nicotinamide pocket mutants affect the transition-state binding of both NADPH and NADH.

Importance of Head and Tail Binding Residues. Studies in AKRs have shown that many of these enzymes display a distinct preference for NADPH due to a salt bridge between the 2'-AMP (tail group) with a conserved Arg or Lys residue. Our studies show that by mutating the nicotinamide binding residues (headgroup) two modes of cofactor binding are revealed. Thus, the interaction between 2'-AMP with the conserved Arg or Lys is not the sole determinant of cofactor binding preference. This is supported by studies with the R276M mutant of 3 α -HSD, in which the salt bridge between Arg 276 and the 2'-phosphate of AMP is eliminated, and as a result the high-affinity binding for NADP(H) is decreased 100-fold. However, these mutants still bind NADP(H) more tightly than NAD(H) by at least 1 order of magnitude (34). This observation suggests the critical need of the head residues to contribute to high-affinity NADP(H) binding and is supported by the changes in K_d^{NADPH} observed in the mutants. The residues that bind the headgroup also define the reaction trajectory in the wild-type enzyme since the mutations affected the transition-state binding energy with both cofactors and introduced a pronounced primary kinetic isotope effect. Our data also suggest that residues without function in ground-state binding could be recruited to play important roles in transition-state binding. The structural basis for the differences observed in binding NADP $^+$ and NAD $^+$ by nicotinamide pocket mutants will have to wait the determination of the E•NAD $^+$ complex structure. Such a complex may be difficult to obtain due to the low binding affinity that exists for NAD(H). The observation that residues in the nicotinamide pocket contribute to different binding modes for NADP(H) and NAD(H) may impact the interpretation of structure–function relationships in many pyridine nucleotide-linked dehydrogenases.

ACKNOWLEDGMENT

We gratefully acknowledge the valuable discussion and technical support of Dr. Paul H. Axelsen and Mr. Joseph M. Jez. We also thank Dr. Jane M. Vanderkooi for the use of the fluorescence spectrophotometers in her laboratory.

REFERENCES

1. Jornvall, H., Persson, B., Krook, M., Atrian, S., Gonzalez-Duarte, R., Jeffery, J., and Ghosh, D. (1995) *Biochemistry* 34, 6003–6013.
2. Duax, W. L., Griffin, J. F., and Ghosh, D. (1996) *Curr. Opin. Struct. Biol.* 6, 813–823.
3. Breton, R., Housset, D., Mazza, C., and Fontecilla-Camps, J. C. (1996) *Structure* 4, 905–915.

4. Bruce, N. C., Willey, D. L., Coulson, A. F. W., and Jeffery, J. (1994) *Biochem. J.* 299, 805–811.
5. Jez, J. M., Bennett, M. J., Schlegel, B. P., Lewis, M., and Penning, T. M. (1997) *Biochem. J.* 326, 625–636.
6. Wilson, D. K., Bohren, K. M., Gabbay, K. H., and Quijcho, F. A. (1992) *Science* 257, 458–460.
7. Bennett, M. J., Schlegel, B. P., Jez, J. M., Penning, T. M., and Lewis, M. (1996) *Biochemistry* 35, 10702–10711.
8. Kersey, W. H., and Wilcox R. B. (1970) *Biochemistry* 9, 1284–1286.
9. Askonas, L. J., Ricigliano, J. W., and Penning, T. M. (1991) *Biochem. J.* 278, 835–841.
10. Hoff, H. G., and Schriefers, H. (1973) *Hoppe-Seyler's Z. Physiol. Chem.* 354, 507–513.
11. Lin, H. K., Jez, J. M., Schlegel, B. P., Peehl, D. M., Pachter, J. A., and Penning, T. M. (1997) *Mol. Endocrinol.* 11, 1971–1984.
12. Pawlowski, J. E., Huizinga, M., and Penning, T. M. (1991) *J. Biol. Chem.* 266, 8820–8825.
13. Deyashiki, Y., Ogasawara, A., Nakayama, T., Nakanishi, M., Miyabe, Y., Sato, K., and Hara, A. (1994) *Biochem. J.* 299, 545–552.
14. Khanna, M., Qin, K. N., Wang, R. W., and Cheng, K. C. (1995) *J. Biol. Chem.* 270, 20162–20168.
15. Miura, R., Shiota, K., Noda, K., Yagi, S., Ogawa, T., and Takahashi, M. (1994) *Biochem. J.* 299, 561–567.
16. Deyashiki, Y., Ohshima, K., Nakanishi, M., Sato, K., Matsuura, K., and Hara, A. (1995) *J. Biol. Chem.* 270, 10461–10467.
17. Bohren, K. M., Page, J. L., Shankar, R., Henry, S. P., and Gabbay, K. H. (1991) *J. Biol. Chem.* 266, 24031–24037.
18. Kubiseski, T. J., and Flynn, T. G. (1995) *J. Biol. Chem.* 270, 16911–16917.
19. Matsuura, K., Tamada, Y., Sato, K., Iwasa, I., Miwa, G., Deyashiki, Y., and Hara, A. (1997) *Biochem. J.* 322, 89–93.
20. Smithgall, T. E., and Penning, T. M. (1988) *Biochem. J.* 254, 715–721.
21. Pawlowski, J. E., and Penning, T. M. (1994) *J. Biol. Chem.* 269, 13502–13510.
22. Jez, J. M., Schlegel, B. P., and Penning, T. M. (1996) *J. Biol. Chem.* 271, 30190–30198.
23. Lowry, O. H., Rosebrough, N. J., Farr, A. J., and Randall, R. J. (1951) *J. Biol. Chem.* 193, 265–275.
24. Smithgall, T. E., and Penning T. M. (1988) *Biochem. J.* 254, 715–721.
25. Leatherbarrow, R. J. (1987) *ENZFITTER: A Non-Linear Regression Data Analysis Program for the IBM PC (and true compatibles)*, BioSoft, Cambridge, U.K.
26. Wilkinson, G. N. (1961) *Biochem. J.* 80, 324–332.
27. Bennett, M. J., Albert, R. H., Jez, J. M., Ma, H., Penning, T. M., and Lewis, M. (1997) *Structure* 5, 799–812.
28. Loewus, F. A., Westheimer, F. H., and Vennesland, B. (1953) *J. Am. Chem. Soc.* 75, 5018–5023.
29. Loewus, F. A., Levy, H. R., and Vennesland, B. (1956) *J. Biol. Chem.* 223, 589–597.
30. Jez, J. M., and Penning, T. M. (1998) *Biochemistry* 37, 9695–9703.
31. Viola, R. E., Cook, P. F., and Cleland, W. W. (1979) *Anal. Biochem.* 96, 334–340.
32. Fersht, A. (1985) *Enzyme Structure and Mechanism* (2nd ed.), pp 301–309, W. H. Freeman and Co., New York.
33. Sem, D. S., and Kasper, C. B. (1993) *Biochemistry* 32, 11548–11558.
34. Ratnam, K., Ma, H., and Penning, T. M. (1999) *Biochemistry*, 38, 7856–7864.
35. Ratnam, K., Ma, H., and Penning, T. M. (1999) *FASEB. J.* 13, A1113.
36. Northrop, D. B. (1977) in *Isotope Effects on Enzyme Catalyzed Reactions* (Cleland, W. W., O'Leary, M. H., and Northrop, D. B., Eds.), p 122, University Park Press, Baltimore, MD.
37. Segel, I. H. (1975) *Enzyme Kinetics*, pp 560–564, John Wiley & Sons, Inc., New York.
38. Grimshaw, C. E., Bohren, K. M., Lai, C.-J., and Gabbay, K. H. (1995) *Biochemistry* 34, 14356–14365.
39. Mesecar, A. D., Stoddard, B. L., and Koshland, D. E., Jr. (1997) *Science* 277, 202–206.
40. Koshland, D. E., Jr., and Nee, K. E. (1968) *Annu. Rev. Biochem.* 37, 359–410.

BI991659O